

# A Methodology of Modelling Fish-like Swim Patterns for Robotic Fish

Jindong Liu and Huosheng Hu

Department of Computer Science, University of Essex, Colchester CO4 3SQ, U.K.

Email: jliua@essex.ac.uk, hhu@essex.ac.uk

**Abstract**— This paper presents a novel modelling methodology for our robotic fish, which considers the relative movement of the tail to the head in order to model variable swimming patterns for robotic fish. It deduces a tail motion function from a fish body motion function and then uses multiple joints to approximate the tail motion function. Three basic swim patterns are modelled and some experiment results are presented to show its feasibility and performance. The proposed method can be used as a general method for any multiple-joint robotic fish.

**Index Terms**— Robotic fish, swim patterns, modelling methodology

## I. INTRODUCTION

The astonishing swimming abilities of fish has inspired many researchers to work on a new kind of aquatic man-made robotic systems, namely *Robotic Fish*. Up to now, majority of research work has been focused on the fish-like propulsion mechanism [1], the fin material [2], remote operation[3] and multi-agent cooperation[4] and the mechanical structures [5]. Although several basic swim movements, called swim patterns, have been realized on robotic fish, little research work has been done to give a general methodology to describe how to model variable swim patterns. In this paper, a novel modelling methodology is proposed to realize the fish-like swim patterns in our robotic fish. It first considers the relative movement of the tail to the head and gives an integrated idea to model variable swimming patterns for robotic fish.

The rest of this paper is organized as follows. Section II presents the structure of the proposed methodology, the content of each module and the relationship between them. Section III addresses three examples which use the methodology to model three swim patterns. In Section IV, an evaluation system is first given to evaluate the modelling performance in robotic fish. Then the experimental results are presented to show the feasibility and performance of three modelled swim patterns. Finally, conclusions and future work are given in Section V.

## II. METHODOLOGY OF MODELLING SWIMMING PATTERNS

The centre issue of modelling fish swimming patterns for robotic fish is to describe the swim pattern by the tail motion relative to the head because all swim patterns have to be implemented through movement of tail joints which move relative to the fish head. To realize fish-like swimming patterns, we proposed a modelling methodology as shown in Fig. 1. The body motion function  $f_B(x, t)$  of a specific swim pattern is obtained from biologists, which models the movement of a

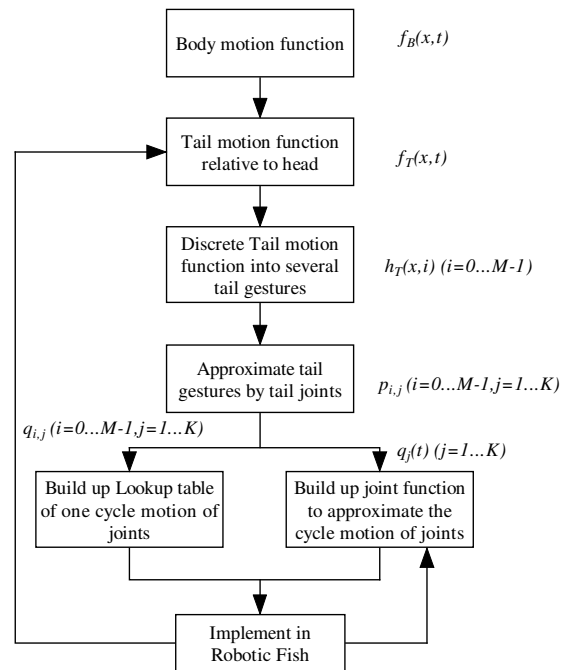


Fig. 1. Methodology of modelling robotic fish swim patterns

whole fish body during swimming. The tail motion function  $f_T(x, t)$  is deduced by subtracting a linear function of head swing from the body motion function. It is a relative motion function between the fish tail and its head. The purpose of generating tail motion functions is to control the tail joints to move in a reference frame, i.e. a head fixed frame, because the interesting part to control is the tail section rather than the whole fish body.

The basic idea of reproducing fish swim patterns on a robotic fish is to apply multiple mechanical joints on the tail to generate the similar tail motion as a real fish does. However, it is difficult and even impossible to deduce the analytic solution of the joint motion function from the tail motion function because of the difficulties of solving a number of sine functions, e.g.,  $f_B(x, t)$ , and polynomial functions, e.g., the constraints of the joint length. So a *digital approximation* method was proposed in [6]. In this method, the tail motion function in one period is discretized into  $M$  tail gestures  $h_T(x, i) (i = 0 \dots M - 1)$  against time. Fig. 2 gives an example of tail gestures of a *cruise-in-straight* swim pattern. In this

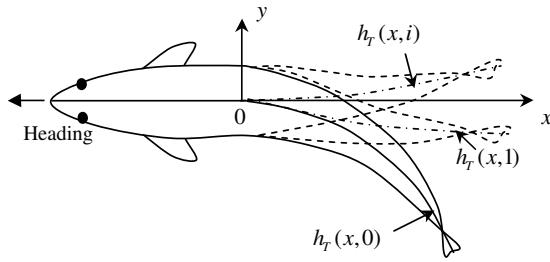


Fig. 2. Tail gestures, i.e., the discretized tail motion function  $h_T(x, i)$  in the head fixed coordinate system.

way, we can mimic the fish swimming by approximating each tail gesture with the rigid linkages between the joints.

Figure 3 shows an example of approximating a tail gesture  $h_T(x, i)$  with four joints. There are four linkages, i.e., (I, II, III, IV), between the joints.  $(x_i, y_i) (i = 0 \dots 3)$  show the position of four joints.  $(x_4, y_4)$  shows the endpoint of the last linkage.  $p_{i,j} (j = 1 \dots 4)$  are the slope angles of the linkages.  $q_{i,j} (j = 1 \dots 4)$  are actual control angles, i.e. turn a joint relative to its anterior linkage. For example,  $q_{i,3}$  means the turning angle of the 3rd joint (at  $(x_3, y_3)$ ) relative to the linkage II for the tail gesture  $h_T(x, i)$ . Thus, the approximation result for a tail motion function  $f_T(x, t)$  can be denoted as  $q_{i,j} (i = 0 \dots M - 1, j = 1 \dots K)$ , here  $K$  is the total number of joints and  $M$  is the number of gestures.

In practice, two methods can be applied to control the joints to turn according to the approximation result  $q_{i,j}$ . The first method is a lookup table method. A lookup table is built to contain all the turning angles of  $q_{i,j} (i = 0 \dots M - 1, j = 1 \dots K)$ . The servo equipped in each joint is controlled to turn by following  $q_{i,j}$  one by one. This method is easy to implement. However, it is hard to revise  $q_{i,j}$  during online learning because the lookup table is constituted by at least 32 knots of each joint to guarantee the smooth approximation. It has to revise the parameters of  $f_T(x, t)$  in order to change  $q_{i,j}$ . The second method is to build a joint motion function  $q_j(t)$  which is a non-linear regression of  $q_{i,j} (i = 0 \dots M - 1)$ .  $q_j(t)$  can be a polynomial function or other non-linear functions, e.g., sine function. Thus, it is convenient to adapt the parameter of swim patterns because  $q_j(t)$  has limited parameters and is readily twisted online. See Section III-A for the details of the regression procedure.

For different swim patterns, the body motion function also varies. Because most previous research has focused on *cruise straight*, the body motion functions of all other swim patterns have not been explored so far. To study these swim patterns, we model *cruise-in-turning* modelled by revising the body motion function of *cruise straight*. For the *sharp turn* swim pattern, there isn't any body motion function revealed by biologists. It is modelled directly from a tail motion function based on our observation of real fish turning.

### III. IMPLEMENTATION SWIM PATTERNS

In our implementation, we divide the carangiform fish swimming motion into several basic swim patterns based

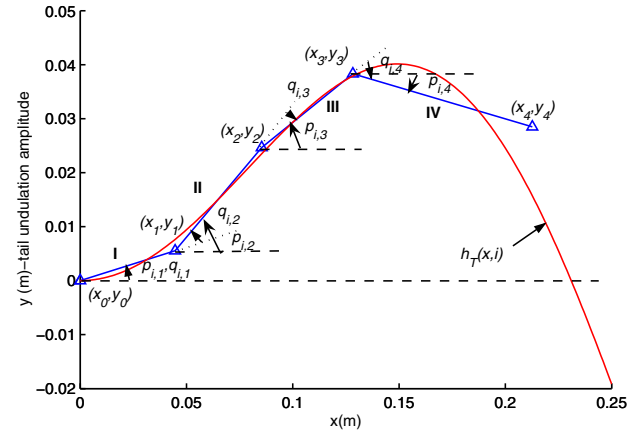


Fig. 3. An example of tail gesture approximation. The original point is the connection between fish head and tail.  $(x_i, y_i)$  is the joint position. It supposes that the tail has four joints in total.

on the observation from biologists and ourselves. We will implement the methodology to realize following swimming patterns:

- *Cruise straight*: The fish swims along a straight line at a constant speed, possibly with small acceleration/deceleration ( $|a| < 0.3L/s^2$ ,  $L$  is the length of fish body). *Cruise straight* belongs to *periodic swimming*. It can be modeled by a time-variant traveling wave function and implemented by approximating the function with the tail joints. See details in Section III-A.
- *Cruise-in-turning*: The fish turns at a small angular speed ( $|\omega| < 0.5\text{rad/s}$ ) but at a constant linear speed. It is one of *periodic swimings* and modelled by the same time-variant traveling wave function as *cruise straight* except that a time-invariant offset wave is added onto the wave function. The approximating method with tail joints is also used for this swim pattern. See details in Section III-B.
- *Sharp turn*: The fish generates a brief and sudden angular acceleration to avoid predators or obstacles. There are two main types of sharp turn according to the fish body shape: *C-shape* and *S-shape*. In the biology literature, there is a term "Fast start" which is divided to two basic motions here: *sharp turn* and *burst*. *sharp turn* is an *unsteady movement*. *C-shape* sharp turn is modelled by a novel time-variant circle function and *S-shape* sharp turn hasn't been modelled by anyone yet. In terms of practical implementation, the approximating method is applied. See details in Section III-C.

In summary, *cruise straight* and *cruise-in-turning* are examples of *periodic swimming*, while *sharp turn* represents *unsteady swimming*.

#### A. Cruise Straight Swim Patterns

The motion of a fish body during *cruise straight* could be described by a travelling wave (1), which was originally

suggested by [7] and is widely used in robotic fish research. The parameter of the fish travelling wave changes depending on the fish types and its kinetics status in water. Here we have the fish body motion function:

$$y = f_B(x, t) = (c_1x + c_2x^2) \sin(kx + \omega t) \quad (1)$$

where the original point is set as the conjunction point between fish head and tail.  $y$  is the transverse displacement of a tail unit;  $x$ -axis is the centre line of the undulation wave of *Cruise Straight*;  $k = \frac{2\pi}{\lambda}$  is the wave number;  $\lambda$  is the wave length;  $c_1$  is the linear wave amplitude envelope;  $c_2$  is the quadratic wave amplitude envelope;  $\omega = 2\pi f$  is the wave frequency;  $t$  is the time.

Fig. 4 shows an example of the fish body function. It shows that the fish undulates its tail to generate the propulsion wave. Following the methodology in Section II, the body motion function must be converted into the tail motion function before the digital approximation. Assume the fish head part, from the nose tip to  $x = 0$  point, is rigid and the gradient of the head is the same as the derivative of Equation (1) at  $x = 0$ . Then the tail movement relative to the head could be expressed by subtracting a linear function  $y = c_3x$ , here  $c_3$  is the gradient of head swing, from the body motion function (1).  $c_3$  can be calculated as the first-order derivative of  $f_B(x, t)$  at  $x = 0$ , i.e.:

$$\begin{aligned} c_3 &= f'_B(x, t) |_{x=0} = (c_1 + 2c_2x) \sin(kx + \omega t) + \\ &\quad (c_1x + c_2x^2)k \cos(kx + \omega t) |_{x=0} \\ &= c_1 \sin(\omega t) \end{aligned} \quad (2)$$

So the tail motion function corresponding to Equation (1) is:

$$\begin{aligned} f_T(x, t) &= f_B(x, t) - c_3x \\ &= (c_1x + c_2x^2) \sin(kx + \omega t) - c_1x \sin(\omega t) \end{aligned} \quad (3)$$

Comparing Fig. 4 and Fig. 5, it is noticeable that the amplitude of the relative motion is larger than the one of body motion. In other words, the tail has to undulate itself with a bigger amplitude than the observed one to achieve the swimming wave because the head sways during swimming. This is a KEY consideration when reproducing real fish swimming on a robotic fish.

After obtaining the tail motion function  $f_T(x, t)$ , the digital approximation can be done and the joint angle  $q_{i,j}$  is calculated (see Fig. 6) given the tail length:  $[l_1, l_2, l_3, l_4] = [0.045, 0.045, 0.045, 0.085]$  m.

In our practical realization of the robotic fish, the series of joint angle  $q_{i,j}$  is regressed to a time-dependent function  $q_j(t)$ , where  $j$  is the index of joints. Because  $q_j(t)$  must be periodic in *periodic swimming* and its shape is similar to a sine function (see Fig. 6), so it can be represented by the Fourier series:

$$q_j(t) = \sum_{n=1}^{\infty} a_{n,j} \sin(n\omega t + \varphi_{n,j}) \quad (4)$$

Generally, only the first index in Equation (4) is chosen to simplify our online learning. The 1st phase of first joint,  $\varphi_{1,1}$ ,

is set to zero without losing generality. So the form of the joint angle to be controlled can be written as follows:

$$q_j(t) = a_j \sin(\omega t + \varphi_j), j = 1 \dots K \quad (5)$$

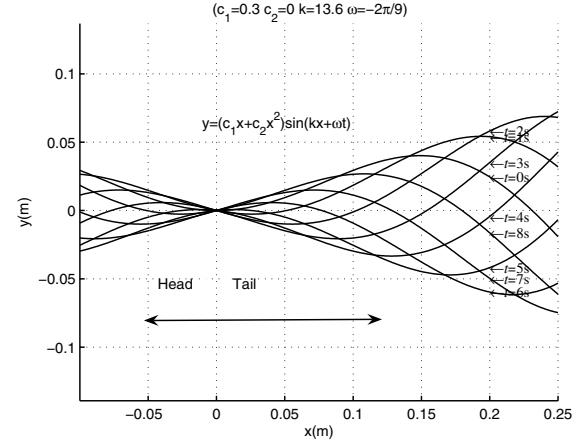


Fig. 4. An example of body motion function.

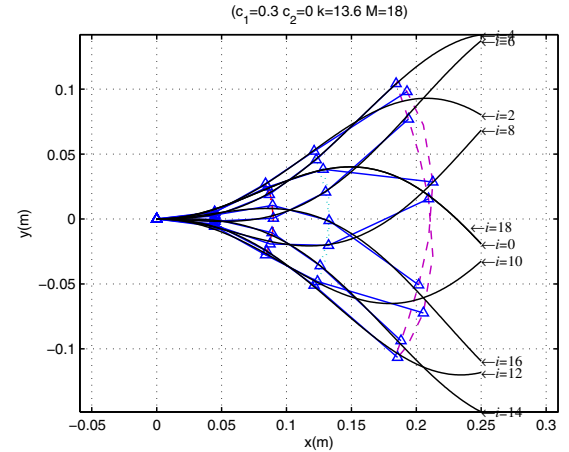


Fig. 5. The approximation result of a 4-joint tail for *cruise straight*

## B. Cruise-in-Turning Swim Patterns

When a fish is performing *Cruise-in-turning*, its body motion function can be modelled by the sum of the body motion function of *cruise straight* and a deflected centre curve, denoted as  $d(x)$ . So the undulation centre of the tail movement becomes a curve rather than a straight line as in *cruise straight*, as shown in Fig. 7. However, nobody has shown the form of  $d(x)$ . Based on our observation of fish swimming, we assume:

$$\begin{aligned} d(x) &= d_1 x^{d_2}, d_2 > 1, x > 0 \\ d_1 &\begin{cases} > 0 & \text{cruise-in-right-turn} \\ < 0 & \text{cruise-in-left-turn} \end{cases} \end{aligned} \quad (6)$$

where  $d_2$  is the curvature factor to control the curvature of the deflected centre and  $d_1$  is the direction factor to control

the turning direction, which is also proportional to the turning angle when  $d_2$  is fixed.

Therefore, the body motion function of *cruise-in-turning* can be written as follows:

$$y = f_B(x, t) = (c_1x + c_2x^2) \sin(kx + \omega t) + d_1x^{d_2} \quad (7)$$

where all the parameters have a similar definition to Equation (1). Actually, it can be viewed as the uniform body motion equation of *cruise straight* and *cruise-in-turning* because it is exactly equal with (1) when  $d_1 = 0$ .

Following the methodology in Section II, the tail motion function corresponding to Equation (7) can be written as:

$$\begin{aligned} f_T(x, t) &= f_B(x, t) - c_3x \\ &= (c_1x + c_2x^2) \sin(kx + \omega t) + d_1x^{d_2} - c_1x \sin(\omega t) \end{aligned} \quad (8)$$

After getting the tail motion function  $f_T(x, t)$ , the digital approximation can be done and the joint angle  $q_{i,j}$  is calculated (see Fig. 8) for practical control. Similar to *cruise in straight*, in practical terms of *cruise-in-turning* on our robotic fish, the joint angle  $q_{i,j}$  is regressed to a time-dependent function  $q_j(t)$ :

$$q_j(t) = a_j \sin(\omega t + \varphi_j) + b_j, j = 1 \dots K \quad (9)$$

### C. C-shape Sharp Turning Swim Patterns

Sharp turning has mainly two kinds: C-shape and S-shape. We first consider the C-shape in which fish bends its tail quickly to one side and the tail shape like a ‘‘C’’ during the bending.

Fig. 9 is a C-shape sharp turn sequence recorded from an adult carp [8]. The shape changing of the tail during a sharp turning can be imagined like that the fish embraces a virtual circle using its flexible tail (see details in our another paper [9]). The virtual circle changes its centre and radius against the turning time. The circumference of the virtual circle determines the tail shape. Based on this observation, a circle function (10) can be written in the head-fixed coordinate

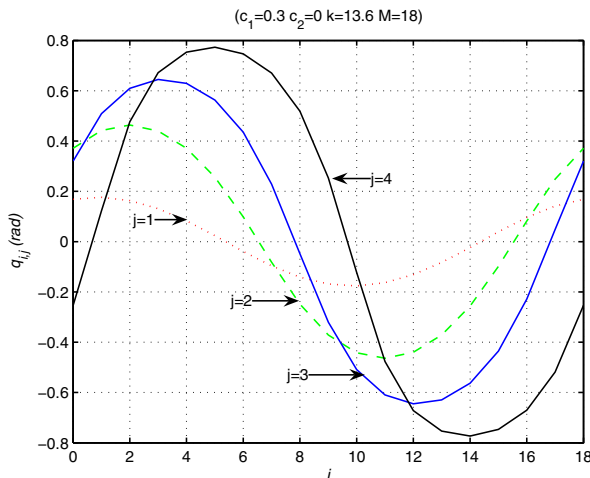


Fig. 6. The joint angle calculated by the digital approximation method for *cruise straight*

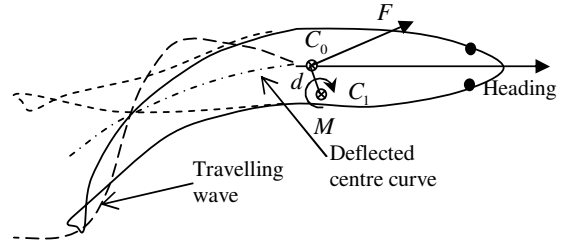


Fig. 7. Model for Cruise-in-turning

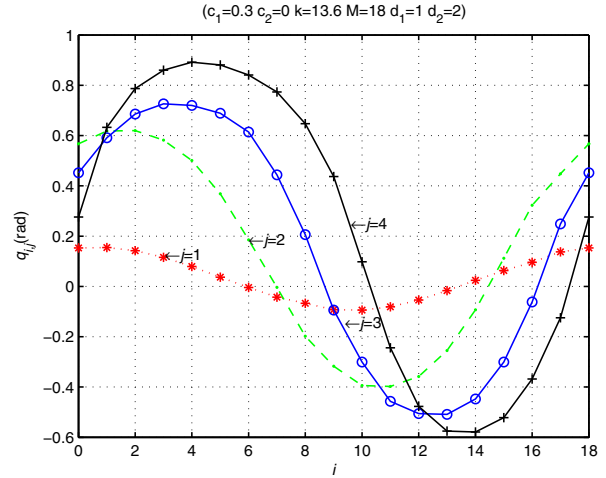


Fig. 8. The joint angle calculated by the digital approximation method for *cruise in right turning*

system. See Fig. 10 for the shape of a virtual circle (in dash line).

$$(x - x_c(t))^2 + (y - y_c(t))^2 = y_c^2(t) \quad (10)$$

where  $x_c(t)$  and  $y_c(t)$  form the changing of the circle centre in terms of time.  $y_c(t)$  is also used for the circle radius because the virtual circle is always tangent to the x-axis. If we get the function of  $x_c(t)$  and  $y_c(t)$ , we can generate a series of circle functions by discretizing time  $t$  into  $(0 \dots M - 1)$ . These circle functions can be viewed as tail gestures  $h_T(x, i)$  (Fig. 2) of the shape tuning. Then the digital approximation method can be used to calculate the turning angles of joints in order to approximate these gestures. Now, the question of modelling the C-shape sharp turning is converted to how to find proper functions of  $x_c(t)$  and  $y_c(t)$ .

So, the form of  $y_c(t)$  is proposed as Equation (11):

$$y_c(t) = \begin{cases} cy_1 + (cy_0 - cy_1) \frac{(t-t_1)^k}{(t_0-t_1)^k} & t \in [t_0, t_1] \\ cy_1 + (cy_1 - cy_2) \frac{(t-t_1)^m}{(t_2-t_1)^m} & t \in [t_1, t_2] \end{cases} \quad (11)$$

where  $k > 1$ ,  $m > 1$  are parameters to decide the feature of the sharp turn such as the tail shape, the bending speed and the maximum bending angle, etc.

So,  $x_c(t)$  can be written as a second-order polynomial equation of  $y_c(t)$  as follows:

$$x_c(t) = \begin{cases} a_{11}y_c^2(t) + a_{12}y_c(t) + a_{13} & t \in [t_0, t_1] \\ a_{21}y_c^2(t) + a_{22}y_c(t) + a_{23} & t \in [t_1, t_2] \end{cases} \quad (12)$$

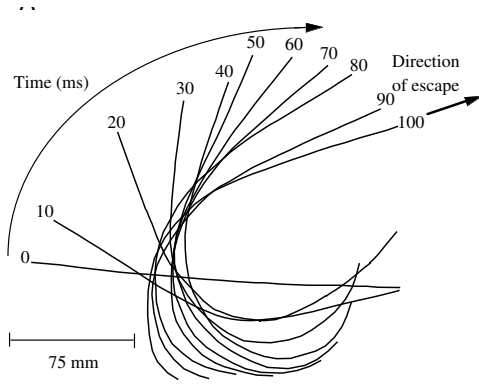


Fig. 9. A C-shape sharp turn sequence recorded from an adult carp [8]

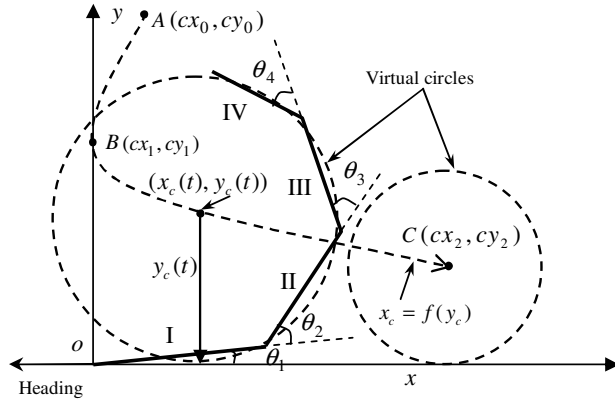


Fig. 10. The virtual circle function of C-shape sharp turning and an example of the approximation result.

where  $a_{ij}$  can be calculated easily if given the coordinates of point  $A$ ,  $B$  and  $C$ .

An example of the trajectory of  $(x_c(t), y_c(t))$  is shown in Fig. 10. A series of virtual circle functions can be obtained now from  $(x_c(t), y_c(t))$ . They are the tail gestures to approximate using the tail linkages. An approximate example is displayed in Fig. 10. Fig. 11 presents the joint angle  $q_{i,j}$  against time. It is clear that there is a sharp increase in the shrink stage ( $t < 15$ ) and a slower decrease in the release stage ( $15 < t < 35$ ). The unit of time  $t$  is 50 ms.

#### IV. EXPERIMENTAL RESULTS AND ANALYSIS

In this section, each designed swim pattern is tested in our real robotic fish, G9 series, including Green G9, Blue G9 and White G9. The experimental tank is 5.5 m in length, 1.7 m in width, and 1.7 m in height with 1.5 m water depth.

##### A. Evaluation System for Swim Patterns

Up to now, most robotic fish projects focused on the bio-hydrodynamics mechanism of the *cruise straight* swim pattern. The corresponding evaluation system [3][10] only considers the factors related to the energy efficiency and the vortex morphology generated from swimming. There are no factors to describe fish-like swim patterns to mimic real fish motion apart

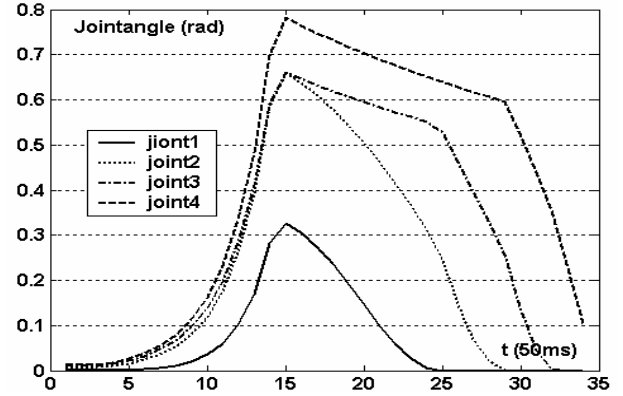


Fig. 11. The joint angle curve in a sharp turn.

from the *cruise straight*. It is necessary to build an evaluation system to evaluate the performance of these swim patterns.

These criterion are selected based on two factors: (i) The morphological feature of real fish swimming, i.e., evaluating how well the robotic fish swims like a real fish. We believe that the swim pattern of real fish is the optimal one after thousands of years of evolution. Therefore, the robotic fish should swim like a real fish. (ii) The kinematic characteristics of swim patterns. They are the explicit factors to gauge the performance of fish swimming. In details, the physical meanings of the factors in the evaluation system are discussed as follows:

- Linear speed  $V_p$  is a kinematic factor to measure the absolute linear speed of *cruise straight*. It is also a basic factor to calculate the Strouhal number below. The swimming speed of fish is often measured in body lengths per second (BL/s), which is calculated by  $V_{BL} = V_p/L$ , where  $L$  is the body length of a robotic fish.  $V_{BL}$  is normally used to compare the maximum speed between different robotic fish.
- Head swing factor  $S_h$  is a morphological factor to evaluate *cruise straight*. It is the ratio between the amplitude of the head tip undulation and the amplitude of the tail tip undulation. Generally, for a carangiform  $S_h$  should be in the range of 0.15 to 0.4. A large  $S_h$  means that a large amount of energy is wasted by the fish head in pushing the water to sides. A small  $S_h$  indicates that the body motion function (1) has wrong parameters and it can not generate fish-like body motion.
- Strouhal number  $St$  is adapted from [10], which was used to characterize the structure of vortex wakes released after the fish tail. It is chosen as a morphological factor here because it is a relative stable factor in range 0.25 to 0.40 [11] for fish representing subcarangiform, carangiform and thunniform modes.
- Turning radius  $r$  is a kinematic factor for both *cruise-in-turning* and *C-shape sharp turning*. It measures the operating range during turning.
- Angular speed  $\omega_t$  and  $\omega_c$  are kinematic factors for *cruise-in-turning* and *C-shape sharp turning*. They gauge the change of fish heading in unit time.

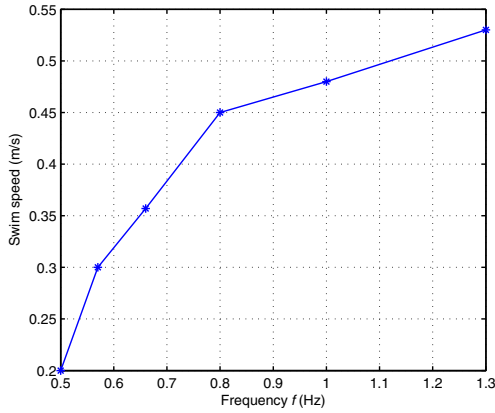


Fig. 12. Relationship between swim speed and tail flapping speed

- Maximum bending angle  $\beta_c$  is both a morphological factor and a kinematic factor for *C-shape sharp turning*. It is around 90 to 120 degrees in a real fish.
- Turning efficiency  $\eta_c$  is a kinematic factor for *C-shape sharp turning*. From its definition of  $\eta_c = \theta_c/\beta_c$ , higher  $\eta_c$  means that the robotic fish achieves a faster turning speed by a smaller turning angle.

### B. Periodic Swimming Pattern

For G9 robotic fish, when tail flapping frequency  $f = 0.5$  Hz, linear speed  $V_p = 0.2$  m/s, head swing factor  $S_h = A_h/A_t = 0.07/0.2 = 0.35$ , Strouhal number  $St = fA_t/V_p = 0.5 * 0.2/0.2 = 0.5$ . It is clear that all morphological factors lie in or near to the desired range. The *cruise straight* swim pattern of the robotic fish is smooth and very similar to a real fish. The relationship between  $f$  and  $V_p$  is shown in Fig. 12, where the maximum linear speed is 0.53 m/s and the corresponding body length speed  $V_{BL} = V_p/L = 0.53/0.6 = 0.9$ . The turning radius  $r = 0.6$  m and angular speed  $\omega_t = 70/11 = 6.36^\circ/s$ .

### C. Unsteady Swimming Movement

Fig. 13 plots the angular speed  $\omega_c$  and turning angle  $\theta_c$  against time  $t$ . The duration of sharp turning is about 2.5 s. In the shrink stage, the turning speed increased to  $130^\circ/s$  quickly from beginning within 1 s, then the robotic fish started the release stage, and finally the speed is decreased to  $0^\circ/s$ . The maximum turning angle is  $105^\circ$  which is achieved at 2 s. The final turning angle is about  $80^\circ$ . This process is quite similar to real fish sharp turning. The average angular speed  $\omega_c = \theta_c/(t_2 - t_0) = 80/2.5 = 32^\circ/s$ . The turning efficiency  $\eta_c = \theta_c/\beta_c = 80/120 = 0.67$ .

## V. CONCLUSION AND FUTURE WORK

In this paper, a novel modelling methodology is developed to realize fish-like swim patterns in our robotic fish. Three basic swim patterns are modelled and some experimental results are presented to show its feasibility and good performance. Our robotic fish has been in the public show in London

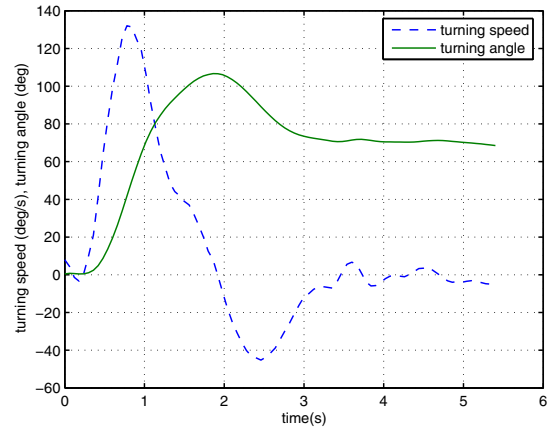


Fig. 13. Performance of C-shape sharp turning

Aquarium since its successful launch on 6 October 2005, and attracted thousands of visitors worldwide.

Our future work will be focused on modelling other swim patterns, such as the S-shape shape turning and realize online learning of control parameters.

### ACKNOWLEDGMENT

This research is funded by London Aquarium. Our thanks also go to Ian Dukes and George Francis at Essex for their contribution toward the project.

### REFERENCES

- [1] K. Naom. Control Performance in the Horizontal Plane of a Fish Robot with Mechanical Pectoral Fins. *IEEE Journal of Oceanic Engineering*, vol. 25(1), 2000:pp. 121–129.
- [2] J. Witting, K. Safak, and G. Adams. SMA Actuators Applied to Biomimetic Underwater Robots. In J. Ayers, J. Davis, and A. Rudolph, eds., *Neurotechnology for Biomimetic Robots*. MIT Press, 2001, pp. 117–136.
- [3] J. Liang. Researchful Development of Underwater Robofish II- Development of a Small Experimental Robofish. *Robot*, vol. 24(3), 2002:pp. 234–238.
- [4] J. Yu, S. Wang, and M. Tan. A simplified Propulsive Model of Biomimetic Robot Fish and Its Realization. *Robotica*, vol. 23, 2005:pp. 101–107.
- [5] S. Guo, T. Fukuda, N. KATO, and K. OGURO. Development of Underwater Microprobe Using IMPF Actuator. In *Proceedings of IEEE International Conference on Robotics and Automation*. IEEE, Leuven, Belgium, May 1998, pp. 1829–1834.
- [6] J. Liu and H. Hu. Building a Simulation Environment for Optimising Control Parameters of an Autonomous Robotic Fish. In *Proceedings of CACSCUK*. Sept 2003, pp. 317–322.
- [7] M. J. Lighthill. Note on the Swimming of Slender Fish. *J. Fluid Mech.*, vol. 9, 1960:pp. 305–317.
- [8] I. L. Y. Spierts and J. L. V. Leeuwen. Kinematics and Muscle Dynamics of C- and S-starts of Carp (*Syprinus Carpio L.*). *Journal of Experimental Biology*, vol. 202, 1999:pp. 393–406.
- [9] J. Liu and H. Hu. Mimicry of Sharp Turning Behaviours in a Robotic Fish. In *Proceedings of IEEE International Conference on Robotics and Automation*. Barcelona, Spain, April 2005, pp. 3329–3334.
- [10] M. Sfakiotakis. Review of Fish Swimming Modes for Aquatic Locomotion. *IEEE Journal of Oceanic Engineering*, vol. 24(2), 1999:pp. 237–252.
- [11] G. S. Triantafyllou, M. S. Triantafyllou, and M. A. Grosenbaugh. Optimal Thrust Development in Oscillating Foils with Application to Fish Propulsion. *Journal of Fluids and Structures*, vol. 7, Feb. 1993:pp. 205–224. doi:10.1006/jfls.1993.1012.